J. theor. Biol. (1996) **179,** 229–242

Complex Periodic Behaviour in a Neural Network Model with Activity-Dependent Neurite Outgrowth

A. van Ooyen and J. van Pelt

Netherlands Institute for Brain Research, Meibergdreef 33, 1105 *AZ Amsterdam, The Netherlands*

(*Received on* 12 *January* 1995, *Accepted in revised form on* 26 *October* 1995)

Empirical studies have demonstrated that electrical activity of the neuron can directly affect neurite outgrowth. High levels of activity cause neurites to retract, whereas low levels allow further outgrowth. Previously we studied networks in which all the cells reacted in the same way on electrical activity. Since experiments have shown that neurons may in fact react differentially, we study in this paper networks in which the range of activity where outgrowth takes place varies among cells. We show that this can lead to complex periodic behaviour in electrical activity and connectivity of individual cells. The precise behaviour depends on the spatial distribution of the cells and the distribution of the outgrowth properties over the cells.

Any other cellular property that adapts slowly to electrical activity such that neuronal activity is attempted to be maintained at a given level, can lead to similar results.

1. Introduction

Electrical activity plays an important role in the development of neurons into functional networks. Many processes that determine connectivity and neuronal function are modulated by electrical activity: e.g. naturally occurring cell death, neurite outgrowth and neuronal morphology, changes in the number and effectiveness of transmitter receptors and ion channels, and synaptic plasticity (for reviews see Fields & Nelson, 1992; Corner, 1994; Van Ooyen, 1994). As a result of these activity-dependent processes, a reciprocal influence exists between neuronal activity (''fast dynamics'') and the development of connectivity and neuronal function (''slow dynamics''). In this article we focus on activity-dependent neurite outgrowth.

A number of studies have demonstrated that neurotransmitters and electrical activity can directly affect neurite outgrowth (for review see Mattson, 1988). Neurites stop growing or even retract under conditions of (high) neuronal activity (Cohan & Kater, 1986; Fields *et al*., 1990; Schilling *et al*., 1991; Grumbacher-Reinert & Nicholls, 1992). Such alterations in outgrowth are mediated by changes in intracellular calcium concentrations ($[Ca^{2+}]_{in}$) (Cohan *et al*., 1987; Kater *et al*., 1988; Mattson, 1988; Kater & Mills, 1991). Depolarization leads to an increase in $[Ca^{2+}]_{in}$, and many aspects of the motility of neurites are regulated by Ca^{2+}. In connection with these observations, the Ca^{2+} theory of neurite outgrowth has been proposed (e.g. Kater *et al*., 1988; 1990), which states that low $[Ca^{2+}]_{in}$ (low level of electrical activity) stimulates outgrowth, higher concentrations cause a cessation of outgrowth, and still higher concentrations (high level of electrical activity) lead to regression of neurites. In addition, outgrowth is also blocked if $[Ca^{2+}]_{in}$ is too low.

We have made a start at unravelling the implications of activity-dependent neurite outgrowth (van Ooyen & van Pelt, 1994a; Van Ooyen *et al*., 1995), and have shown, among other things, that this process, in combination with a neuronal response function possessing some form of firing threshold—a property which gives rise to a hysteresis effect—is sufficient to cause a transient overproduction (i.e. ''overshoot'') with respect to connectivity in a

developing neural network. Overshoot phenomena constitute a general feature of nervous system development, and occur with respect to e.g. number of synapses and neuritic length (for references see van Ooyen & van Pelt, 1994a).

Previously we studied networks in which the critical level of electrical activity (or $[Ca^{2+}]_{in}$) above which the neurites of a cell retract, was the same for all cells. However, this level is in fact different for different classes of neurons (Guthrie *et al*., 1988; Kater *et al*., 1988, 1990). What constitutes a high level of electrical activity for one neuron may actually fall within the permissive outgrowth range of another. Such differences could be due to different initial or basal levels of intracellular Ca^{2+} or to different Ca^{2+} buffering capacities (Kater *et al*., 1988). In the light of this, we consider in the present study networks made up of cells that have such differences in outgrowth properties.

The model is described in Section 2. A brief summary of previous results is given in Section 3.1. The periodic behaviour with respect to connectivity and electrical activity in cells within a (large) network is described in Section 3.2. This behaviour will be qualitatively explained in Section 3.3 using a series of simplified models. In Section 3.4 it is shown that the same results are obtained when neurite outgrowth is replaced by any other slow activity-dependent process that acts to stabilize neuronal electrical activity levels ('homeostasis'). Preliminary results of this study have been reported in van Ooyen & van Pelt (1994b).

2. The Model

The model is used as a tool to explore the possible consequences of activity-dependent neurite outgrowth for network behaviour, in a general and qualitative sense. The initially disconnected neurons organize themselves into a network under the influence of endogenous electrical activity only. Growing neurons are modelled as expanding neuritic fields, and the outgrowth of each neuron depends upon its own level of activity. Neurons become connected when their neuritic fields overlap. In this study, all connections are taken to be excitatory. The model is inspired in part by tissue cultures of dissociated cerebral cortex cells (Van Huizen *et al*., 1985, 1987; Van Huizen, 1986; Ramakers *et al*., 1991), which become organized into a network by neurite outgrowth and synaptogenesis without the influence of external input.

The model is the same as the one used in previous studies (van Ooyen & van Pelt, 1994a, b; van Ooyen *et al*., 1995), and is studied both analytically and by means of numerical solution, employing the variable time step Runge–Kutta integrator provided by Press *et al*. (1988). The simplified models (Sections 3.3 and 3.4) are analysed using GRIND (De Boer, 1983).

2.1. NEURON MODEL

To describe neuronal activity, the shunting model (Grossberg, 1988) is used, in which excitatory inputs drive the membrane potential towards a finite maximum or saturation potential. For a purely excitatory network, after transformation to dimensionless equations (e.g. Carpenter & Grossberg, 1983; van Ooyen *et al*., 1995), this model becomes

$$\frac{dX_i}{dT} = -X_i + (1 - X_i) \sum_{j=1}^{N} W_{ij} F(X_j), \qquad (1)$$

where X_i represents the (time averaged) membrane potential of cell i, scaled between the saturation potential (set to 1) and the resting membrane potential (set to 0), N is the total number of excitatory cells, T is the time in units of the membrane time constant, W_{ij} is the connection strength between neuron j and i ($W_{ij} \geqslant 0$; W_{ij} is defined in Section 2.2), and

$$F(X) = \frac{1}{1 + e^{(\theta - X)/\alpha}}, \qquad (2)$$

where $F(X)$ is the mean firing rate (with its maximum set to 1), α determines the steepness of the function and θ represents the firing threshold. The low firing rate when the membrane potential is sub-threshold can be considered as representing spontaneous activity, arising from threshold or membrane potential fluctuations (for references see van Ooyen *et al*., 1995).

2.2. OUTGROWTH AND CONNECTIVITY

Neurons are randomly placed on a two-dimensional surface. Each neuron is given a circular "neuritic field", the radius of which is variable. When two such fields overlap, both neurons become connected with a strength proportional to the area of overlap:

$$W_{ij} \equiv A_{ij} S, \qquad (3)$$

where $A_{ij} = A_{ji}$ is the amount of overlap ($A_{ii} = 0$), representing the total number of synapses formed reciprocally between neurons i and j, while S represents the average synaptic strength. In this

abstraction, no distinction has been made between axons and dendrites, but in Section 3.4 we consider whether or not such asymmetry affects the results.

Since the effect of activity on outgrowth is mediated by intracellular calcium, and since the firing of action potentials leads to increases in $[Ca^{2+}]_{in}$ (see Section 1), we take the outgrowth of each individual cell to be dependent upon its firing rate:

$$\frac{dR_i}{dT} = \rho G(F(X_i)), \tag{4}$$

where R_i is the radius of the circular neuritic field of neuron i, and ρ determines the rate of outgrowth. Note that connection strength is not directly modelled but is a function of neuritic field size. The function G has a zero crossing at $u = \varepsilon_i$ such that

$$\begin{cases} \text{for } u < \varepsilon_i & G(u) > 0 \\ \text{for } u > \varepsilon_i & G(u) < 0 \\ \text{for } u = \varepsilon_i & G(u) = 0. \end{cases} \tag{5}$$

Equation (5) is a phenomenological description of the theory of Kater *et al*. (see Section 1) to the effect that relatively low electrical activity (i.e. below "setpoint" ε_i) allows neurite outgrowth, while sufficiently high activity (i.e. above ε_i) causes neurites to retract (excluding that outgrowth also does not seem to take place at very low levels of activity). To take into account the empirical observation that the level of electrical activity (or $[Ca^{2+}]_{in}$) above which the neurites of a cell retract is not the same for all cells (see Section 1), ε_i is allowed to differ among cells.

For the network model (Sections 3.1 and 3.2), the following growth function is used:

$$G(F(X_i)) = 1 - \frac{2}{1 + e^{(\varepsilon_i - F(X_i))/\beta}}, \tag{6}$$

where β determines the steepness of G. This function remains in the bounded range $\langle -1, 1 \rangle$.

Outgrowth of neurons is on a timescale of days or weeks (e.g. Van Huizen *et al*., 1985, 1987; Van Huizen, 1986; Schilling *et al*., 1991), so that connectivity is quasi-stationary on the timescale of membrane potential dynamics (i.e. ρ small). To avoid unnecessarily slowing down the simulations, ρ is chosen as large as possible while maintaining the quasi-stationary approximation. In the simulations of the network model, we use $\rho = 0.0001$. As nominal values for the other parameters, for both the network model and the simplified models, we choose $\theta = 0.5$, $\alpha = 0.10$, $\beta = 0.10$. For ε, all possible values are considered.

3. Results

3.1. IDENTICAL OUTGROWTH FUNCTION

In this section we briefly summarize the previous results relevant for this study. The variations in **W** take place much more slowly than those in X, so that **W** can in a first approximation be considered as a parameter of the system. For a given **W** in a purely excitatory network, the equilibrium points are solutions of [see eqn (1)]

$$0 = -X_i + (1 - X_i) \sum_{j=1}^{N} W_{ij} F(X_j) \quad \forall i. \tag{7}$$

If all the cells have the same ε_i, and the variations in X_i are small (relative to $\bar{X}$, the average membrane potential of the network), the average connection strength $\bar{W}$ can be written as a function of $\bar{X}$ (van Ooyen & van Pelt, 1994a):

$$\bar{W} = \frac{\bar{X}}{(1 - \bar{X})F(\bar{X})} \quad 0 \leqslant \bar{X} < 1. \tag{8}$$

The slow movement of the system determined by the dynamics in connectivity takes place along the manifold defined by eqn (8) [See Fig. 1(a)]. It is the so-called slow manifold, and is the same as the equilibrium manifold of $\bar{X}$ (defined by $d\bar{X}/dT = 0$) for $\bar{W}$ as a parameter of the system. The manifold is S-shaped ("hysteresis loop"), which underlies the emergence of overshoot and oscillations (further see the caption of Fig. 1).

3.2. NETWORK OF CELLS HAVING DIFFERENT OUTGROWTH FUNCTIONS

For a network in which ε is different for different cells, the resulting network behaviour depends also on the spatial distribution of the cells (e.g. random as opposed to regular) as well as on the distribution of the ε values over the cells.

Especially if the spatial distribution of cells is such that all of them become strongly connected to many of their neighbours (as will happen with a regular distribution of cells), not all of the cells need to have an ε in the non-oscillatory range (see Fig. 1) in order for both the network as a whole and the individual cells to show an absence of oscillations (in both connectivity and electrical activity). For example, in a network consisting of sixteen regularly placed cells, in which only five cells have $\varepsilon = 0.8$ (which, if all cells had this value, would cause an overshoot in connectivity and no subsequent oscillations), and the rest have $\varepsilon = 0.4$ (which, if all cells had this value, would cause sustained oscillations in connectivity and electrical activity) still shows a "normal" overshoot

sequence, without any oscillations (also not in any of the individual cells). With a different, less central distribution of these five cells, the individual cells show oscillations between quiescent and activated state with different amplitudes [see Fig. 2(a3–5)]. Note that the network as a whole still shows overshoot with only small oscillations in connectivity in the final state [Fig. 2(a1)].

Especially if the spatial distribution of cells is such that they do not all become equally strongly connected to their neighbours (as will happen with a random distribution), complex periodic behaviour can occur with individual cells displaying oscillations that differ in frequency and amplitude [see Fig. 2(b1–4), (c1, 2)]. The network as a whole will then show an overshoot with oscillations in connectivity (and electrical activity) in the final state, the amplitude of which will vary among different networks, depending on the distribution of ε values.

3.3. SIMPLIFICATIONS

To derive a simplification, let us consider two cell types, X and Y, that differ only in their respective ε values, ε_X and ε_Y. As a spatial configuration that can occur in the network, we consider two X cells and two Y cells that, for simplicity, are placed in such a way that the $X(Y)$ cells are identical to each other with respect to the overlap of their neuritic fields with those of the other cell type (Fig. 3), so that, starting with the same initial conditions, their dynamics will be the same: each $X(Y)$ cell is, as it were, connected to itself.

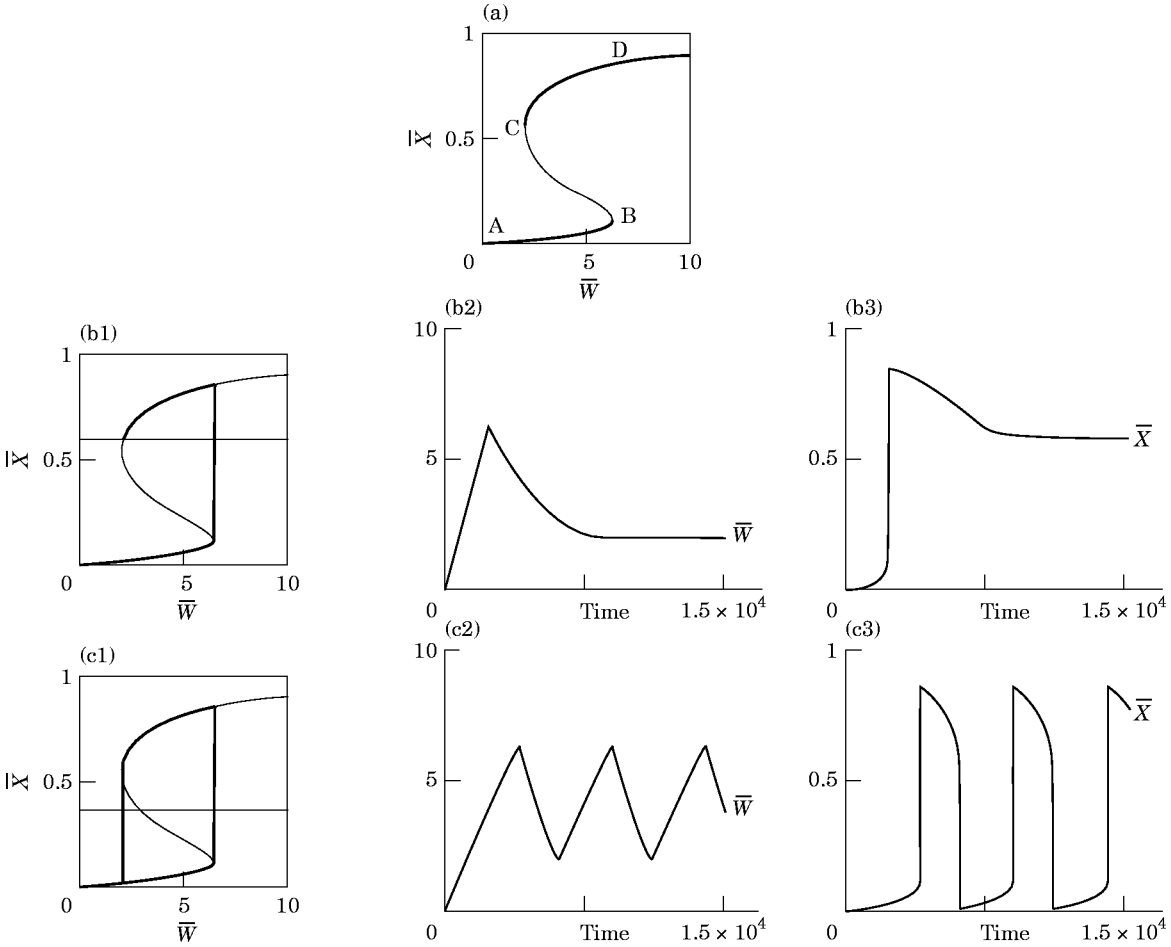

FIG. 1. Hysteresis. (a) The S-shaped slow manifold of $\bar{X}$ ($d\bar{X}/dT = 0$) in the ($\bar{W}$, $\bar{X}$)-plane ($\bar{W} = (1/N)\,\Sigma_{i=1,j=1}^{N} W_{ij}$), as defined by eqn (8). When $\bar{W}$ is regarded as a parameter, states on BC are unstable, while the others are stable (bold lines). The horizontal lines in (b1) and (c1) indicate $\bar{X} = F^{-1}(\varepsilon)$ (F^{-1} is the inverse of F). Above and below that line, $\bar{W}$ decreases and increases, respectively [see eqn (6)]. The connectivity, $\bar{W}$, is quasi-stationary on the time scale of membrane potential dynamics, and, starting at A, $\bar{X}$ will follow the branch AB, until it reaches B, where it jumps to the upper branch. (b1) If the intersection point of the horizontal line is on CD, $\bar{W}$ decreases again, and a developing network has to go through a phase in which $\bar{W}$ is higher than in the final situation (i.e. "overshoot" in $\bar{W}$). The trajectory is shown as a bold line. In (b2) $\bar{W}$, and in (b3) $\bar{X}$ is shown against time. (c1–3) An ε such that the intersection point is on BC, results in regular oscillations.

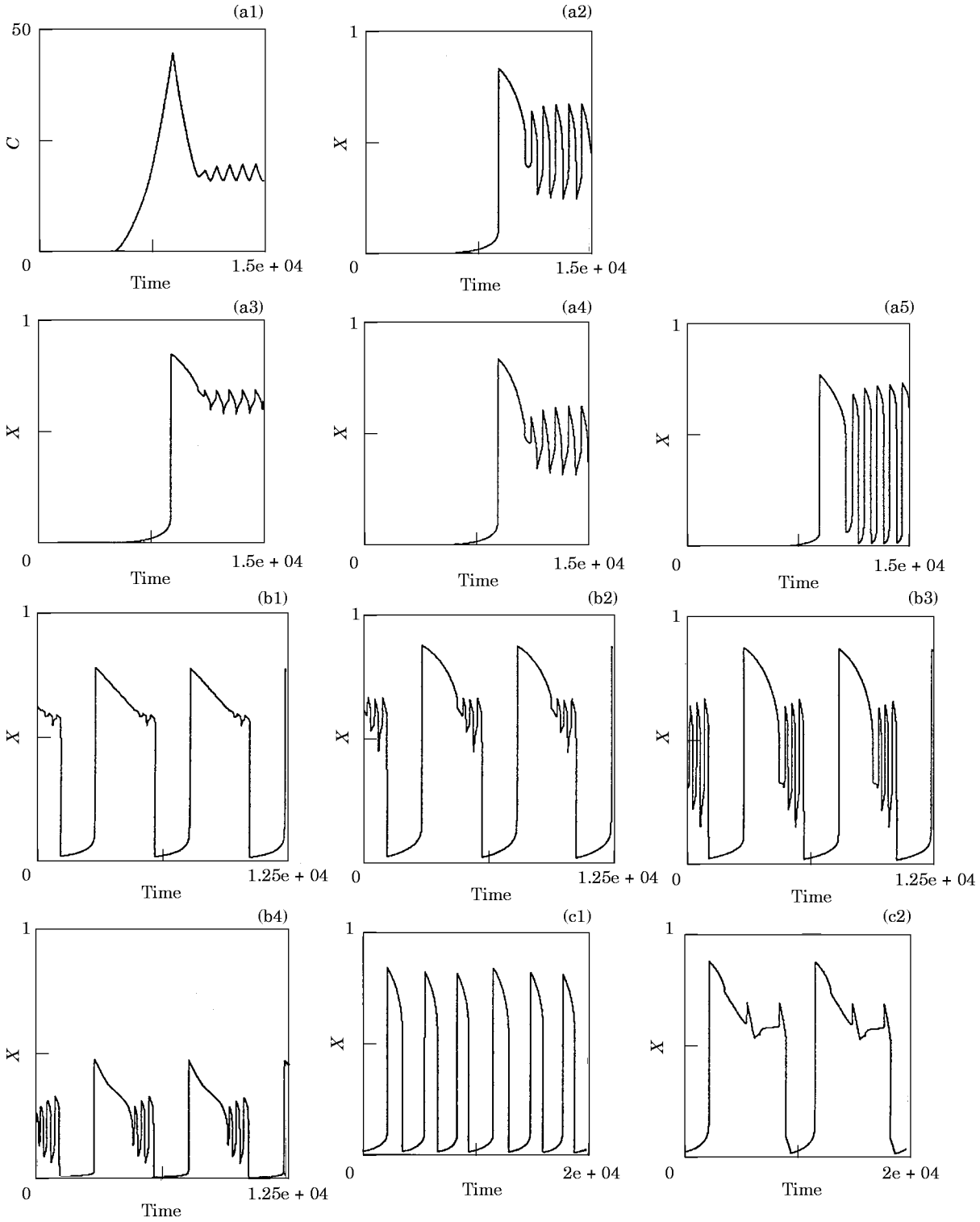

FIG. 2. Behaviour of individual cells in a network [governed by eqns (1) and (6)]. (a) Network of 16 cells placed on a grid. Five cells have $\varepsilon = 0.8$, the rest has $\varepsilon = 0.4$. (a1) Overshoot in total connectivity ($C = \Sigma_{i=1,j=1}^{N} A_{ij}$). (a2) Average membrane potential in the network. (a3–5) Membrane potential of three different cells. The cell of (a4) has $\varepsilon = 0.4$, the rest has $\varepsilon = 0.8$. (b) Membrane potential of four different cells in a network of 16 randomly placed cells in which ε is uniformly distributed between 0.05 and 0.8. In all figures the initial transients are skipped. (b1) $\varepsilon = 0.65$. (b2) $\varepsilon = 0.67$. (b3) $\varepsilon = 0.36$. (b4) $\varepsilon = 0.10$. (c) Network consisting of a group of two cells (both have $\varepsilon = 0.68$) neighbouring to a large group of 19 cells (all have $\varepsilon = 0.15$). Initial transients are skipped. (c1) $\varepsilon = 0.15$. (c2) $\varepsilon = 0.68$.

For the connection strengths between the cells, we have

$$\begin{aligned} W_{XX} &= \varphi(R_X)S \\ W_{YY} &= \varphi(R_Y)S \\ W_{XY} &= W_{YX} = \psi(R_X, R_Y)S = \xi(W_{XX}, W_{YY}), \end{aligned} \tag{9}$$

where $W_{XX}(W_{YY})$ is the connection strength between the two $X(Y)$ cells with radius $R_X(R_Y)$, W_{XY} is the connection strength between an X and Y cell, φ and ψ are functions determining the area of overlap between the cells [also see eqn (3)], and $S > 0$ represents synaptic strength. For the dynamics of W (under the restriction that $W > 0$) we have

$$\begin{aligned} \frac{\mathrm{d}W_{XX}}{\mathrm{d}T} &= S\varphi'(R_X)\frac{\mathrm{d}R_X}{\mathrm{d}T} \\ \frac{\mathrm{d}W_{YY}}{\mathrm{d}T} &= S\varphi'(R_Y)\frac{\mathrm{d}R_Y}{\mathrm{d}T}. \end{aligned} \tag{10}$$

Since the outgrowing circular neuritic field is just one of the possible ways to model connectivity, we are not interested in the precise form of φ and ξ, which should not affect the essential findings. We therefore took simple functions φ and ξ, which indeed turned out to be sufficient for capturing the essential behaviour. We take φ such that $\varphi'(R) = a > 0$. Thus,

$$\begin{aligned} \frac{\mathrm{d}W_{XX}}{\mathrm{d}T} &= Sa\frac{\mathrm{d}R_X}{\mathrm{d}T} = qG(X) \\ \frac{\mathrm{d}W_{YY}}{\mathrm{d}T} &= Sa\frac{\mathrm{d}R_Y}{\mathrm{d}T} = qG(Y), \end{aligned} \tag{11}$$

were $q = a\rho S$. The growth function G is taken to depend directly on the membrane potential instead of on the firing rate (this gives the same results, also in the network, see van Ooyen & van Pelt, 1994a), and, since the precise form of G is not crucial as long as it obeys eqn (5), the simplest form of G is used: $G(X) = \varepsilon_X - X$, $G(Y) = \varepsilon_Y - Y$. For ξ we take

$$W_{XY} = p(W_{XX} + W_{YY}), \tag{12}$$

where p incorporates the spatial component (i.e. distance between the cells, see Fig. 3) that can cause the connection strength between the two $X(Y)$ cells to be different from that between cell X and Y (if $p = 0.5$ and $W_{XX} = W_{YY}$, all connection strengths are the same). Thus, the complete model becomes

$$\begin{aligned} \frac{\mathrm{d}X}{\mathrm{d}T} &= -X + (1 - X)[W_{XX}F(X) + W_{XY}F(Y)] \\ \frac{\mathrm{d}Y}{\mathrm{d}T} &= -Y + (1 - Y)[W_{YY}F(Y) + W_{YX}F(X)] \\ \frac{\mathrm{d}W_{XX}}{\mathrm{d}T} &= q(\varepsilon_X - X) \\ \frac{\mathrm{d}W_{YY}}{\mathrm{d}T} &= q(\varepsilon_Y - Y) \\ W_{XY} &= W_{YX} = p(W_{XX} + W_{YY}). \end{aligned} \tag{13}$$

In all the simulations, we use $q = 0.005$. An alternative interpretation of eqn (13) is that X and Y represent the average membrane potential of a population of X and Y cells, respectively (provided the variations among the individual cells are small relative to the average values, see van Ooyen & van Pelt, 1994a), and the W's the average connection strength impinging on a given cell.

The complex periodic behaviour seen in the network arises also in this simplified model. As already mentioned, the precise form of the functions φ, ψ (and ξ) is not essential. For example, if we take $\varphi(R_X) \sim R_X^2$, $\varphi(R_Y) \sim R_Y^2$ and $\psi(R_X, R_Y) \sim R_X R_Y$ [with $\mathrm{d}R_X/\mathrm{d}T = \rho G(X)$ and $\mathrm{d}R_Y/\mathrm{d}T = \rho G(Y)$] very similar results are obtained. In order to understand the basis for the occurrence of the complex behaviour, let us consider some further simplifications. The various simplified models, as described hereafter, also correspond to different spatial distributions of cells in the full network model, for which such simplifications are warranted (see Section 3.3.5).

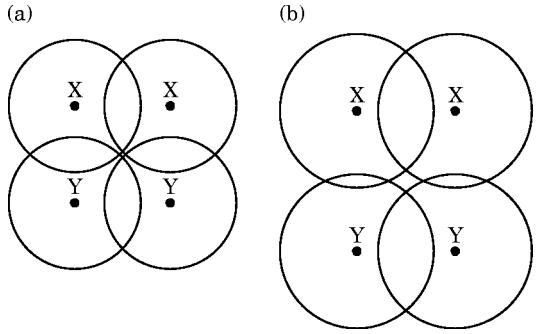

FIG. 3. The spatial distribution of the cells determines the relative connection strengths. (a) The connection strength between both $X(Y)$ cells is the same as that between an X and Y cell. (b) The connection strength between both $X(Y)$ cells is different from that between an X and Y cell.

3.3.1. *Model I*

To study the effect of input on an X or Y cell, the following model is used:

$$\begin{aligned} \frac{\mathrm{d}X}{\mathrm{d}T} &= -X + (1 - X)[W_{XX}F(X) + I] \\ \frac{\mathrm{d}W_{XX}}{\mathrm{d}T} &= q(\varepsilon_X - X). \end{aligned} \tag{14}$$

There is only one cell type, and the input from Y in

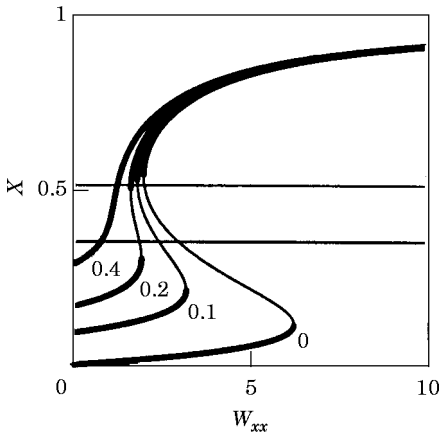

FIG. 4. External input makes the hysteresis loop of the slow manifold of $X(dX/dT = 0)$ smaller [see eqn (14)]. Shown are the manifolds for $I = 0$, 0.1, 0.2 and 0.4. The horizontal lines indicate the position of $\varepsilon_X = 0.51$ and $\varepsilon_X = 0.35$, respectively. The meaning of the bold lines is as in Fig. 1(a).

eqn (13) is replaced by a constant input I. This enables us to show how the slow manifold of X, and consequently the behaviour of the system, changes under input. Increasing I causes the turning points of the manifold to move towards each other (in both W_{XX} and X) so that the hysteresis loop becomes smaller and finally disappears (Fig. 4).

For $\varepsilon_X = 0.51$ and $I = 0$, for example, the system described by eqn (14) shows oscillations (in W_{XX} and X) which become smaller for $I > 0$. They have disappeared when $I = 0.2$, under which condition the system shows overshoot (starting with $W_{XX} = 0$). For $\varepsilon_X = 0.35$ the system does not show overshoot no matter what the value of I. If ε_X is such that overshoot occurs for $I = 0$, it will also occur for higher values of I, until the hysteresis loop has disappeared.

3.3.2. *Model II*

Instead of a fixed input I, we now let the input to X be generated by Y. We further fix W_{XY} at a non-zero value, and set $W_{YX} = 0$ so that Y behaves independently of X. Thus,

$$\begin{aligned}
\frac{dX}{dT} &= -X + (1 - X)[W_{XX}F(X) + W_{XY}F(Y)] \\
\frac{dY}{dT} &= -Y + (1 - Y)W_{YY}F(Y) \\
\frac{dW_{XX}}{dT} &= q(\varepsilon_X - X) \qquad (15) \\
\frac{dW_{YY}}{dT} &= q(\varepsilon_Y - Y) \\
W_{XY} &= C.
\end{aligned}$$

To describe the behaviour of this and subsequent models, we shall distinguish a number of different cases that are characterized by ε_X and ε_Y and the resulting behaviour in X and Y *when* X *and* Y *are uncoupled* (i.e. when $W_{XY} = W_{YX} = 0$, which gives two independent equations identical to eqn (14) with $I = 0$). Thus, $\varepsilon_X(\varepsilon_Y)$ can be such that there is a stable point on the lower branch of the slow manifold of $X(Y)$ [stable-lb], a stable point on the upper branch (stable-ub), or an unstable point, which causes regular oscillations. In Fig. 1(a) this corresponds to an intersection point on branch AB, CD or BC, respectively. The *coupling* between X and Y can give rise to complex periodic behaviour. In the following we give an inventory of the qualitatively different behaviours we found. In the figures, manifolds of $X(Y)$ defined as $dX/dT = 0$ ($dY/dT = 0$) *for a given value of* $Y(X)$, are drawn in the $(W, X)[(W, Y)]$ plane.

(1) ε_Y = stable-lb or stable-ub, ε_X = stable-lb or stable-ub.
Since there is no influence from X to Y, Y goes to ε_Y independently of ε_X, and $W_{XY}F(Y)$ becomes constant. That is, we end up with the same situation as in eqn (14) with $I > 0$. The influence of Y does not change the stability of the points: X always goes to a stable point [Fig. 5(a)].

(2) ε_Y = sable-lb or stable-ub, ε_X = unstable.
Again $W_{XY}F(Y)$ becomes constant, and depending on the value of $W_{XY}F(\varepsilon_Y)$
   (a) the oscillations in X (and W_{XX}) become smaller [Fig. 5(b)] or
   (b) the oscillations disappear completely (i.e. stable point).

(3) ε_Y = unstable, ε_X = stable-ub or stable-lb.
In this case Y oscillates, and independently of X. Because of the nature of these oscillations (i.e. being the result of W_{YY} varying very slowly relative to the dynamics of Y), Y essentially jumps between values on the lower branch (quiescent state) and values on the upper branch (activated state), while spending very little time at values in between. As is illustrated in Fig. 4, the manifold of X is different for a low or a high input (i.e. Y). In Fig. 5 the manifold of X is drawn for Y at the quiescent state (represented by $Y = 0$) and the activated state (represented by $Y = 0.7$). Since X attempts to follows its manifold, any time Y jumps from quiescent to activated state or vice versa, the behaviour of X can, to a good approximation, be described as jumping between these two

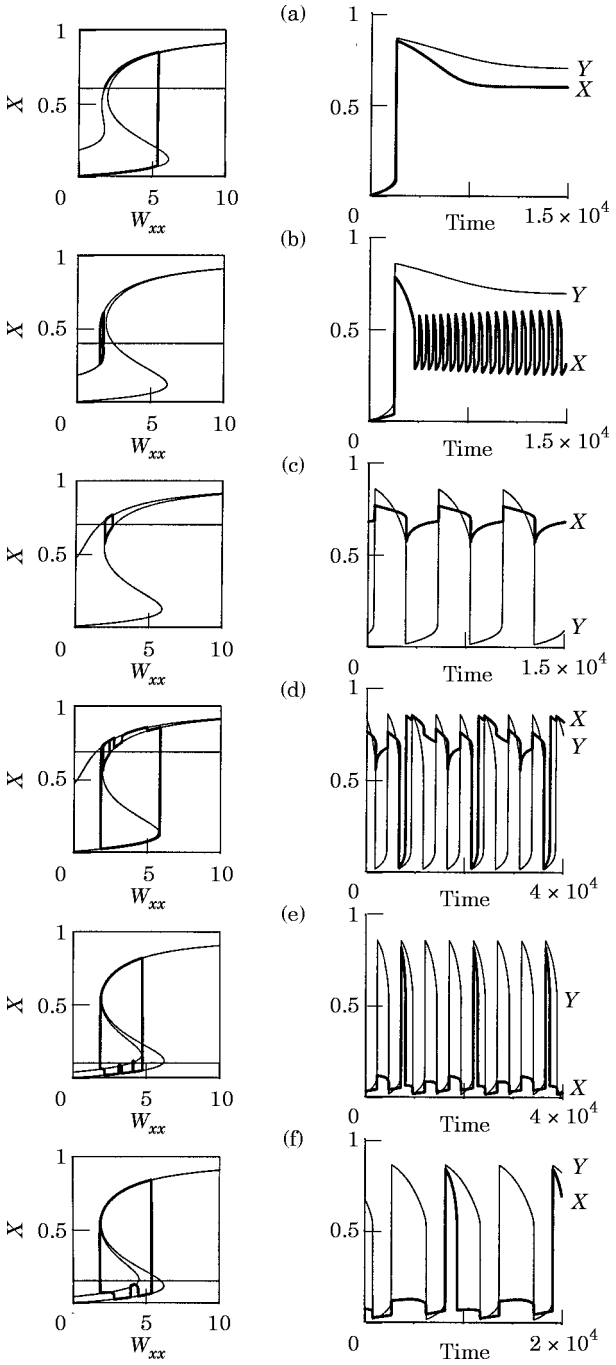

FIG. 5. Behaviour of the model described by eqn (15) for different values of ε_X and ε_Y. In each figure of the first column, the bold line is the trajectory of the system in the (W_{XX}, X)-plane, the thin horizontal line indicates the value of ε_X, and the thin S-shaped lines are the manifolds of X defined as $dX/dT = 0$ for $Y = 0$ (lower curve) and $Y = 0.7$ (upper curve), respectively. In each corresponding figure of the second column, the behaviour of X (bold line) and Y is plotted against time. (a) $\varepsilon_Y = 0.7$, $\varepsilon_X = 0.6$, $W_{XY} = 0.25$. Note that the transition from quiescent to activated state takes place not at the turning point of the slow manifold but at a lower W_{XX} value because of the additional drive from Y. (b) $\varepsilon_Y = 0.7$, $\varepsilon_X = 0.4$, $W_{XY} = 0.25$. (c) $\varepsilon_Y = 0.4$, $\varepsilon_X = 0.7$, $W_{XY} = 1.0$. (d) $\varepsilon_Y = 0.4$, $\varepsilon_X = 0.685$, $W_{XY} = 1.0$. (e) $\varepsilon_Y = 0.4$, $\varepsilon_X = 0.1$, $W_{XY} = 0.045$. (f) $\varepsilon_Y = 0.5$, $\varepsilon_X = 0.15$, $W_{XY} = 0.05$. In all figures, except those of (a) and the time plot of (b), the initial transients are skipped.

manifolds (also see Fig. 6(a), in which the complete 3D picture is given). The oscillations in Y can cause X to make

(a) small oscillations (i.e. X stays at the upper branch if ε_X = stable-ub [Fig. 5(c)] or at the lower branch if ε_X = stable-lb);
(b) oscillations between quiescent and activated state, at the same frequency as those of Y;
(c) oscillations between quiescent and activated state, at a lower frequency than those of Y [Fig. 5(d, e)].

4. ε_Y = unstable, ε_X = unstable.
X will oscillate between quiescent and activated state
(a) at the same frequency of Y or
(b) at a lower frequency of Y [Fig. 5(f)].

In all cases, ε_X and ε_Y determine not only whether or not oscillations occur when the cells are uncoupled, but also the relative speed with which X and Y move along their slow manifolds. Together with the strength of the interaction, W_{XY}, this determines the precise form of the oscillations when the cells are coupled. In Fig. 5(c), for example, Y drops to the quiescent state at a moment that X has reached a value such that X will not drop to the lower branch when Y is low. It does drop down when ε_X is only slightly smaller [as in Fig. 5(d)].

3.3.3. *Model III*

In the following model, X also influences Y, and the only difference from eqn (13) is that $W_{XY} = W_{YX}$ is kept constant. Thus

$$\frac{dX}{dT} = -X + (1 - X)[W_{XX}F(X) + W_{XY}F(Y)]$$

$$\frac{dY}{dT} = -Y + (1 - Y)[W_{YY}F(Y) + W_{YX}F(X)]$$

$$\frac{dW_{XX}}{dT} = q(\varepsilon_X - X \tag{16}$$

$$\frac{dW_{YY}}{dT} = q(\varepsilon_Y - Y)$$

$$W_{XY} = W_{YX} = C.$$

Note that, since the model is symmetrical in X and Y, the behaviour we find with ε_X = unstable and ε_Y = stable-ub, for example, is the same as with ε_Y = unstable and ε_X = stable-ub, interchanging X and Y.

(1) ε_Y = stable-lb or stable-ub, ε_X = stable-lb or stable-ub.
As in the previous models, the influence of X on

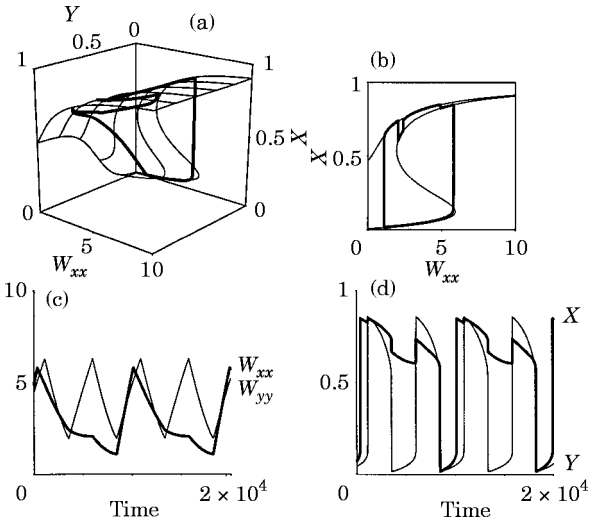

FIG. 6. Behaviour of the model described by eqn (15) for $\varepsilon_Y = 0.4$, $\varepsilon_X = 0.6$, $W_{XY} = 1.0$. Initial transients are skipped. (a) The bold line is the trajectory of the system in (W_{XX}, X, Y)-space. The thin lines are the manifolds of X defined as $dX/dT = 0$ for different values of Y. (b) The bold line is the trajectory of the system in the (W_{XX}, X)-plane. The thin lines are the manifolds of X defined as $dX/dT = 0$ for $Y = 0$ (lower curve) and $Y = 0.7$ (upper curve), respectively. (c) W_{XX} (bold line) and W_{YY} against time. (d) X (bold line) and Y against time.

Y and vice versa does not change the stability of the points: X and Y will always go to stable points. The interesting cases are those with one or both of the ε's unstable.

(2) ε_X = unstable, ε_Y = stable-ub.
   (a) if W_{XY} is large enough Y can make X to go to a stable point;
   (b) with a smaller W_{XY}, X continues to oscillate while, since in contrast to the previous model X also influences Y, Y will oscillate as well, either remaining on the upper branch [Fig. 7(a1–3)] or
   (c) if ε_Y is somewhat smaller, eventually falling down, together with X, to the lower branch [Fig. 7(b1–4)]. The periodicity of this pattern is determined by ε_Y: a slightly higher value results in a longer period [Fig. 7(c)], and a slightly smaller ε_Y results in a shorter period [Fig. 7(d)]. For some values, the period length is no longer constant: extremely long periods alternate "chaotically" with much shorter ones (not shown);
   (d) if ε_X is such that only if Y is close to ε_Y, ε_X is in the oscillatory region, a type of behaviour as illustrated in Fig. 7(e1–3) can be seen: Y moves slowly towards ε_Y and, when it is close enough, X suddenly drops down to the lower branch, as a result of which Y also falls. A lower value of ε_Y makes the process faster, resulting in a shorter period;
   (e) a kind of hybrid situation between Fig. 7(b3) and Fig. 7(e3) is seen in Fig. 7(f2). Because the relative speed with which X and Y move along their branches is now different, Y does initially not drop down to the low branch of its manifold but is just "rescued" by the high branch, so that X can still make several oscillations. The relative speed with which X and Y move (which can be altered by changing ε_X and ε_Y) determines the number of these oscillations. W_{XY} determines the period of these oscillations: the lower W_{XY}, the larger the period [Fig. 7(g)].

(3) ε_X = unstable, ε_Y = stable-lb
   (a) for low ε_Y, Y makes small oscillations staying on the lower branch of its manifold, while X oscillates between quiescent and activated state;
   (b) if ε_Y is higher, Y can also make oscillations between quiescent and activated state, at the same frequency as those of X or
   (c) at a lower frequency [Fig. 7(h1, 2)].

(4) ε_X = unstable, ε_Y = unstable.
   As in the previous model, Y will oscillate between quiescent and activated state
   (a) at the same frequency of X or
   (b) at a lower frequency of X.

3.3.4. *Full model*

The last step to eqn (13) is to have W_{XY} depend upon W_{XX} and W_{YY}, instead of being constant as in eqn (16). With W_{XY} variable, we found the whole range of behaviours as described for model III (with p ranging from 0.01 to 0.3). No qualitatively different behaviours could be found, possibly because the changes in W_{XY} are mostly, via W_{XX} and W_{YY}, parallel to those in X and Y, so that for the effective interactions [i.e. $W_{XY}F(Y)$ and $W_{YX}F(X)$] a constant value for W_{XY} does not affect the system very much.

3.3.5. *Comparison with network model*

A network consisting of a small group of cells of one type (characterized by its ε value) bordering to a much larger group of cells of another type, can, because of the large difference in cell number, be compared to simplified model II, in which cell Y (representing the largest population in the network) influences the other cell X, but not the other way around. In a network of this structure, the same patterns of periodic behaviour can be found as in the

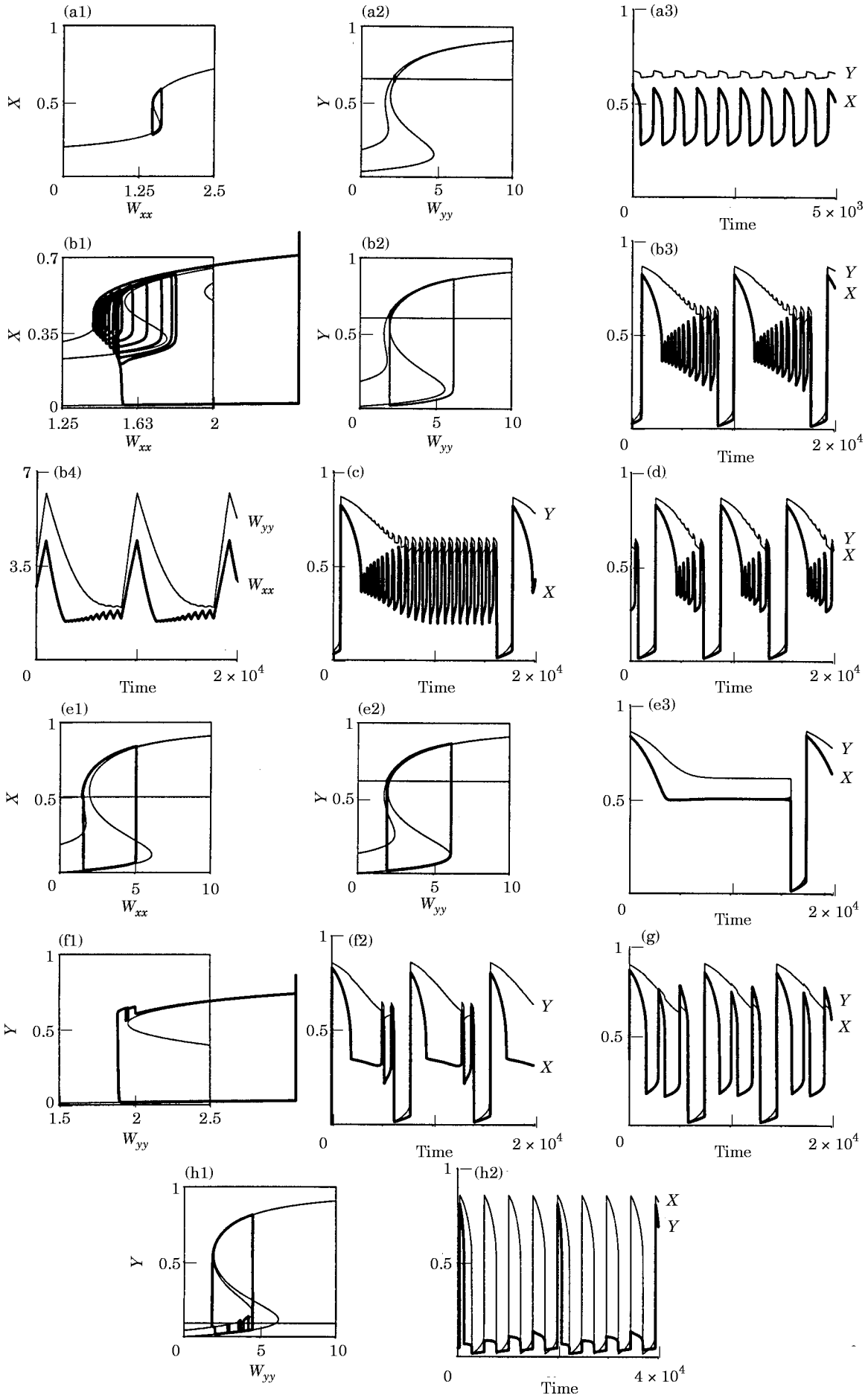

FIG. 7.

simplified model: compare, for example, Fig. 5(d) with Fig. 2(c1, 2). Also the behaviour of simplified model III compares well with the patterns found in the network: for example, compare Fig. 7(a3) with Fig. 2(a3, 4), and Fig. 7(b3, d) with Fig. 2(b1–3). Thus, the interactions in the simplified models are sufficient to capture the essentials of the behaviours found in the network. Under point 2 of both simplified models II and III it is described that with a strong enough connection strength, the oscillations become smaller or disappear if the ε value of the other cell is in the stable region. This underlies the observation that when cells in a network become strongly connected to many of their neighbouring cells, the oscillations become smaller or disappear entirely if only a small proportion of the cells have an ε value in the stable region. Also the fact that complex periodic behaviour can occur especially when not all the cells become equally strongly connected to their neighbours, can be understood from the fact that a large interaction strength (a large W_{XY} in the simplified models) with a neighbouring cell that happens to have an ε value in the stable region would reduce the size of the oscillations or let them disappear.

3.4. GENERALIZATION

In the previous sections we have considered neurite outgrowth, which is an example of a slow activity-dependent process that attempts to stabilize neuronal activity by adapting an intrinsic cellular property. Another example of such a general process is postsynaptic receptor adaptation. After prolonged exposure to its own neurotransmitter, a receptor can become desensitized (e.g. Schwartz & Kandel, 1991). Also the number of receptors can be regulated, with down-regulation following an increase, and up-regulation following a decrease in electrical activity. For example in adult rat neocortex, an increase in neuronal activity or agonist stimulation decreases the number of AMPA receptors (a type of glutamate receptors) (Shaw & Lanius, 1992). Such control of receptor number and sensitivity may be regarded as a form of homeostasis of neuronal activity (Shaw & Lanius, 1992, also see Turrigiano *et al*., 1994).

The following general model is used to study this process:

$$\begin{aligned}
\frac{dX}{dT} &= -X + (1-X)w_X[s_{XX}F(X) + s_{XY}F(Y)] \\
\frac{dY}{dT} &= -Y + (1-Y)w_Y[s_{YY}F(Y) + s_{YX}F(X)] \\
\frac{dw_X}{dT} &= g(\varepsilon_X - X) \\
\frac{dw_Y}{dT} &= g(\varepsilon_Y - Y).
\end{aligned} \tag{17}$$

In this model the number of connections, or synapses, (s_{XX}, s_{YY}, s_{XY} and s_{YX}) is fixed, whereas w_X (w_Y) is variable, e.g. representing the number or effectiveness of the receptors of $X(Y)$. In general, $w_X(w_Y)$ represents any intrinsic (postsynaptic) cellular property that determines the effectiveness of all the cell's incoming connections. Thus, the variable that controls connection strength is not assigned to the interaction between two particular cells, but to the cell itself, so that, for a given cell, the strength of all its incoming connections is affected in the same way. The dynamics of $w_X(w_Y)$ is such that neuronal activity is attempted to be maintained at a given level (ε_X and ε_Y, respectively). For simplicity we assume that $s_{XX} = s_{YY}$, and $s_{XY} = s_{YX}$, and transform eqn (17) into

$$\begin{aligned}
\frac{dX}{dT} &= -X + (1-X)W_X[F(X) + pF(Y)] \\
\frac{dY}{dT} &= -Y + (1-Y)W_Y[F(Y) + pF(X)] \\
\frac{dW_X}{dT} &= q(\varepsilon_X - X) \\
\frac{dW_Y}{dT} &= q(\varepsilon_Y - Y),
\end{aligned} \tag{18}$$

FIG. 7. Behaviour of the model described by eqn (16) for different values of ε_X, ε_Y and W_{XY}. In each of the time plots the bold line indicates X [W_{XX} in (b4)] and the thin line Y [W_{YY} in (b4)], except in (h2). In each of the (W_{XX}, X) [(W_{YY}, Y)]-planes, the thin lines are the manifolds of $X(Y)$ defined as $dX/dT = 0$ ($dY/dT = 0$) for a given value of $Y(X)$; these values will be denoted below. The bold line in each plane is the trajectory of the system. In all figures the initial transients are skipped. (a) $\varepsilon_Y = 0.65$, $\varepsilon_X = 0.4$, $W_{XY} = 0.3$. (a1) $Y = 0.65$. (a2) $X = 0.3$ (lower curve) and $X = 0.6$ (upper curve). (b) $\varepsilon_Y = 0.6$, $\varepsilon_X = 0.4$, $W_{XY} = 0.3$. (b1) $Y = 0$ (lower curve), $Y = 0.6$ (middle curve) and $Y = 0.8$ (upper curve). (b2) $X = 0.2$ (lower curve), $X = 0.6$ (upper curve). (c) $\varepsilon_Y = 0.604$, $\varepsilon_X = 0.4$, $W_{XY} = 0.3$. (d) $\varepsilon_Y = 0.56$, $\varepsilon_X = 0.4$, $W_{XY} = 0.3$. (e) $\varepsilon_Y = 0.61$, $\varepsilon_X = 0.5$, $W_{XY} = 0.3$. (e1) $Y = 0$ (lower curve), $Y = 0.61$ (upper curve). (e2) $X = 0$ (lower curve), $X = 0.5$ (upper curve). (f) $\varepsilon_Y = 0.58$, $\varepsilon_X = 0.35$, $W_{XY} = 0.3$. (f1) $X = 0$. (g) $\varepsilon_Y = 0.58$, $\varepsilon_X = 0.35$, $W_{XY} = 0.15$. (h) $\varepsilon_Y = 0.09$, $\varepsilon_X = 0.4$, $W_{XY} = 0.05$. (h1) $X = 0$ (lower curve), $X = 0.7$ (upper curve). (h2) X and Y (bold line) against time.

where

$$W_X = w_X s_{XX}$$
$$W_Y = w_Y s_{YY}$$
$$p = \frac{s_{XY}}{s_{XX}} = \frac{s_{YX}}{s_{YY}} \qquad (19)$$
$$q = g s_{XX} = g s_{YY}$$

Note that compared with eqn (13), W_{XY} and W_{YX} are missing. An interpretation of eqn (18) in terms of neurite outgrowth would be that only the dendrites grow in an activity-dependent manner, while the axons do not react to electrical activity, and thus remain constant. In analogy to eqn (13), X and Y can also be interpreted as representing the average membrane potential of a population of X and Y cells, respectively.

In order to study the effect of input onto a cell, we will consider, in analogy to eqn (14), the following equation:

$$\frac{dX}{dT} = -X + (1 - X)W_X[F(X) + I], \qquad (20)$$

where $pF(Y)$ is replaced by a constant input I. As with eqn (14), increasing I causes the turning points of the manifold of X to move towards each other, so that the hysteresis loop becomes smaller and finally disappears [Fig. 8(a)]. The only difference with Fig. 4 is that all the manifolds start in ($W_X = 0$, $X = 0$) because I has no effect when $W_X = 0$. Since the effect of I on the form of the manifolds is the same as with eqn (14), the system described by eqn (18) can be expected to show the entire range of behaviours as described for model III and eqn (13), as indeed it does [for examples see Fig. 8(b–d)]. The assumptions we made for s_{XX}, s_{YY}, s_{XY} and s_{YX} are not crucial for these results.

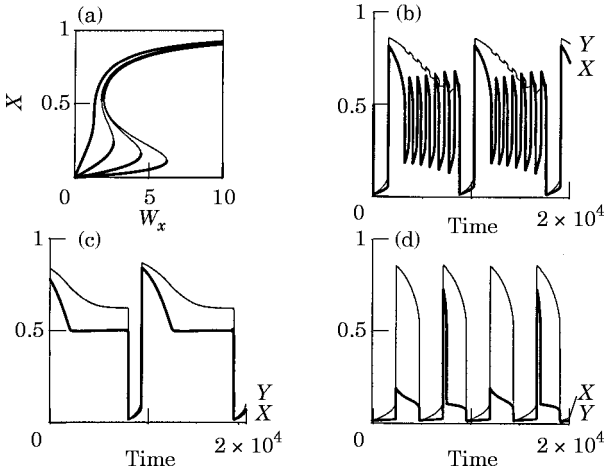

FIG. 8. (a) External input makes the hysteresis loop of the slow manifold of $X(dX/dT = 0)$ smaller [see eqn (20)]. Shown are the manifolds for $I = 0$, 0.01, 0.05 and 0.25. The meaning of the bold lines is as in Fig. 1(a). (b–d) Behaviour of the model described by eqn (18). (b) $\varepsilon_Y = 0.6$, $\varepsilon_X = 0.4$, $p = 0.1$. X (bold line) and Y against time. (c), $\varepsilon_Y = 0.62$, $\varepsilon_X = 0.5$, $p = 0.18$. X (bold line) and Y against time. (d) $\varepsilon_Y = 0.09$, $\varepsilon_X = 0.4$, $p = 0.05$. Y (bold line) and X against time.

4. Conclusions and Discussion

We have demonstrated that in a purely excitatory network composed of cells with differing neurite outgrowth properties (i.e. the level of electrical activity above which retraction occurs varies), the individual cells can exhibit complex periodic behaviour, in both outgrowth and electrical activity, on the timescale of neurite outgrowth. In the full network model, the spatial distribution of the cells can create connectivity patterns that allow for such complex periodic behaviour to occur.

In the previously studied networks (van Ooyen & van Pelt, 1994a; van Ooyen *et al.*, 1995), in which the critical level of electrical activity above which the neurites of a cell retract was the same for all cells, a transient overproduction in connectivity occurred during development. As shown in this paper, this overshoot phenomenon also occurs if the network is made up of cells with differing outgrowth properties (probably a more realistic situation), although in the final state the level of network connectivity may oscillate to a variable extent. Thus, overshoot appears to be a robust phenomenon.

Inclusion of inhibitory cells can be expected to lead to even richer dynamic properties. In van Oss & van Ooyen (1995) it is shown that, even if all cells have the same intrinsic outgrowth properties, activity-dependent outgrowth in the presence of inhibitory cells can lead, among other things, to an interesting type of slow bursting oscillations.

Note that the periodic behaviour described in this paper is not the result of inhibition, of external drive or of transmission delays between cells (e.g. Babloyantz & Destexhe, 1991; Destexhe & Gaspard, 1993). Essential for its occurrence are: (i) a cellular variable that adapts slowly to electrical activity (electrical activity is here the fast variable) whereby activity levels above a specified "setpoint" lead to alterations in the slow variable such that activity decreases, while activity levels below that setpoint lead to the slow variable being altered such that activity increases; (ii) different setpoints for different cells; and (iii) a hysteresis relationship between the slow variable and the average electrical activity in the

network. This last condition can thus also be met in cases where hysteresis emerges as a property of only a large collection of cells (see e.g. Rose & Siebler, 1993). In our model, hysteresis is already present in two inter-connected excitatory cells, and hinges upon (a) the firing rate function having a threshold for transition to a higher firing level and (b) low but non-zero values for sub-threshold membrane potentials. Conditions (a) and (b) are met by, for example, a sigmoidal firing rate function [the exact values of the parameters θ and α of the firing rate function are not crucial; also see van Ooyen & van Pelt (1994a) and Pakdaman *et al*. (1994)].

For the above mentioned analysis and qualitative results to be valid, it is not necessary that the slow process be very much slower than the fast process: for example, with $q = 0.1$ (with a time constant of 1 for the neuronal dynamics), analysis in terms of slow manifolds is still warranted. The precise pattern, however, can be affected by q: a lower value than the one used, for example, results in more "fast" oscillations within the pattern of Fig. 7(b3).

Provided that conditions (i), (ii) and (iii) are met, similar results will be obtained if the fast process (i.e. neuronal activity) is coupled, instead of to neurite outgrowth, to any other slow cellular process that acts to stabilize neuronal activity. For example, slow changes in ion channels that determine the firing properties of a cell [in the model there is also a hysteresis relationship between electrical activity (X) and the firing threshold (θ)], and changes in neurotransmitter receptor sensitivity, as was examined in Section 3.4. A similar situation is described in Carpenter & Grossberg (1983), where a model of circadian rhythms is presented consisting of a four-dimensional fast-slow process in which the fast membrane potentials (described by shunting equations) interact with slowly accumulating chemical transmitter pools. The period of the rhythms is determined by the transmitter accumulation rate.

Since conditions (i), (ii) and (iii) for the generation of complex periodic behaviour are rather general, one might expect to see such oscillations in many different systems [for examples also see Murray (1989) and Rinzel & Ermentrout (1989)]. In tissue cultures of hippocampal neurons, for example, slow oscillations in neurite outgrowth have been observed (S. B. Kater, personal communication). Another example is the variability in firing rate on the order of several minutes, or even slower, which have been observed in tissue cultures of cerebral cortex cells (Ramakers *et al*., 1990; Nuijtinck *et al*., in preparation) as well as *in vivo* (e.g. Mirmiran & Corner, 1982). These fluctuations are usually associated with relatively long-lasting transients of network activity (so-called slow waves, recorded as field potentials) in the range of tens or hundreds of milliseconds, which alternate with periods of minimal activity (for references see van Ooyen *et al*., 1992b). Such patterns in which periods of increased network activity alternate with periods of minimal activity can, together with spontaneously firing cells to trigger network activity, be generated by slowly adapting processes, such as calcium-dependent potassium channels that act to hyperpolarize the cell after repeated firing (van Ooyen *et al*., 1992a).

REFERENCES

Babloyantz, A. & Destexhe, A. (1991). Mapping of spatio-temporal activity of networks into chaotic dynamics: thalamo-cortical networks. In: *Artificial Neural Networks* 1, *Proceedings of the International Conference on Artificial Neural Networks*, *Espoo* (*ICANN*'91) (Kohonen, T., Mäkisara, K., Simula, O. & Kangas, J. eds), pp. 139–144, Elsevier.

Carpenter, G. A. & Grossberg, S. (1983). A neural theory of circadian rhythms: the gated pacemaker. *Biol. Cybern*. **48,** 35–59.

Cohan, C. S. & Kater, S. B. (1986). Suppression of neurite elongation and growth cone motility by electrical activity. *Science* **232,** 1638–1640.

Cohan, C. S., Connor, J. A. & Kater, S. B. (1987). Electrically and chemically mediated increases in intracellular calcium in neuronal growth cones. *J. Neurosc*. **7,** 3588–3599.

Corner, M. A. (1994). Reciprocity of structure-function relations in developing neural networks: the Odyssey of a self-organizing brain through research fads, fallacies and prospects. In: *The Self-Organizing Brain*: *From Growth Cones to Functional Networks*. *Progress in Brain Research* Vol. 102 (Van Pelt, J., Corner, M. A., Uylings, H. B. M., Lopes da Silva, F. H. eds), pp. 3–31.

De Boer, R. J. (1983). GRIND: Great Integrator Differential Equations. University of Utrecht, The Netherlands: Bioinformatics Group.

Destexhe, A. & Gaspard, P. (1993). Bursting oscillations from a homoclinic tangency in a time delay system. *Physics Letters A* **173,** 386–391.

Fields, R. D., Neale, E. A. & Nelson, P. G. (1990). Effects of patterned electrical activity on neurite outgrowth from mouse neurons. *J. Neurosc*. **10,** 2950–2964.

Fields, R. D. & Nelson, P. G. (1992). Activity-dependent development of the vertebrate nervous system. *Int. Rev. Neurobiol*. **34,** 133–214.

Grossberg, S. (1988). Nonlinear neural networks: principles, mechanisms, and architectures. *Neural Networks* **1,** 17–61.

Grumbacher-Reinert, S. & Nicholls, J. (1992). Influence of substrate on retraction of neurites following electrical activity of leech Retzius cells in culture. *J. Exp. Biol*. **167,** 1–14.

Guthrie, P. B., Mattson, M. P., Mills, L. R. & Kater, S. B. (1988). Calcium homeostasis in moluscan and mammalian neurons: neuron-selective set-point of calcium test concentration. *Soc. Neurosc. Abstr*. **14,** 582.

Kater, S. B., Mattson, M. P., Cohan, C. & Connor, J. (1988). Calcium regulation of the neuronal growth cone. *Trends in Neurosc*. **11,** 315–321.

Kater, S. B., Guthrie, P. B. & Mills, L. R. (1990). Integration by the neuronal growth cone: a continuum from neuroplasticity to neuropathology. In: *Progress in Brain Research*, *Vol*. 86, *Molecular and Cellular Mechanisms of Neuronal Plasticity in Normal Aging and Alzheimer's Disease* (Coleman, P. D., Higgins, G. A. & Phelps, C. H. eds), pp. 117–128.

KATER, S. B. & MILLS, L. R. (1991). Regulation of growth cone behaviour by calcium. *J. Neurosc*. **11,** 891–899.

MATTSON, M. P. (1988). Neurotransmitters in the regulation of neuronal cytoarchitecture. *Brain Research Reviews* **13,** 179–212.

MIRMIRAN, M. & CORNER, M. A. (1982). Neuronal discharge patterns in the occipital cortex of developing rats during active and quiet sleep. *Dev. Brain Res*. **3,** 37–48.

MURRAY, J. D. (1989). *Mathematical Biology*, pp. 130–137, Springer–Verlag.

PAKDAMAN, K., VAN OOYEN, A., HOUWELING, A. R. & VIBERT, J.-F. (1994). Hysteresis in a two neuron-network: basic characteristics and physiological implications. In: *Artificial Neural Networks* 1, *Proceedings of the International Conference on Artificial Neural Networks*, *Sorrento* (*ICANN*'94) (Marinaro, M. and P. G. Morasso, P. G. eds), pp. 162–165, Springer–Verlag.

PRESS, W. H., FLANNERY, B. P., TEUKOLSKY, S. A. & VETTERLING, W. T. (1988). *Numerical Recipes in C*, *the Art of Scientific Computing*. Cambridge: Cambridge University Press.

RAMAKERS, G. J. A., CORNER, M. A. & HABETS, A. M. M. C. (1990). Development in the absence of spontaneous bioelectric activity results in increased burst firing in cultures of dissociated cerebral cortex. *Expl. Brain Res*. **79,** 157–166.

RAMAKERS, G. J. A., RAADSHEER, F. C., CORNER, M. A., RAMAEKERS, F. C. S. & VAN LEEUWEN, F. W. (1991). Development of neurons and glial cells in cerebral cortex, cultured in the presence or absence of bioelectric activity: Morphological observations. *Eur. J. Neurosci*. **3,** 140–153.

RINZEL, J. & ERMENTROUT, G. B. (1989). Analysis of neural excitability and oscillations. In: *Methods in Neuronal Modeling*: *from Synapses to Networks*, *Cambridge*, (Koch, C. & Segev, I. eds), Chapter 5, pp. 135–169, MIT Press.

ROSE, G. & SIEBLER, M. (1993). Phase transition effects in spike activity that depend on the degree of connectivity in neural networks. World Congress on Neural Networks 1993, International Neural Network Society Annual Meeting, Portland, Vol. IV, pp. 440–442.

SCHILLING, K., DICKINSON, M. H., CONNOR, J. A. & MORGAN, J. I. (1991). Electrical activity in cerebellar cultures determines Purkinje cell dendritic growth patterns. *Neuron* **7,** 891–902.

SCHWARTZ, J. H. & KANDEL, E. R. (1991). Synaptic transmission mediated by second messengers. In: *Principles of Neural Science* (Kandel, E. R., Schwartz, J. H. & Jessell, T. M. eds), pp. 173–193, Prentice-Hall International Inc.

SHAW, C. & LANIUS, R. A. (1992). Cortical AMPA receptors: age-dependent regulation by cellular depolarization and agonist stimulation. *Dev. Brain Res*. **68,** 225–231.

TURRIGIANO, G., ABBOTT, L. F. & MARDER, E. (1994). Activity-dependent changes in the intrinsic properties of cultured neurons. *Science* **264,** 974–977.

VAN HUIZEN, F., ROMIJN, H. J. & HABETS, A. M. M. C. (1985). Synaptogenesis in rat cerebral cortex is affected during chronic blockade of spontaneous bioelectric activity by tetrodotoxin. *Dev. Brain Res*. **19,** 67–80.

VAN HUIZEN, F. (1986). Significance of bioelectric activity for synaptic network formation. PhD Thesis, University of Amsterdam.

VAN HUIZEN, F., ROMIJN, H. J., HABETS, A. M. M. C. & VAN DEN HOOFF, P. (1987). Accelerated neural network formation in rat cerebral cortex cultures chronically disinhibited with picrotoxin. *Exp. Neurol*. **97,** 280–288.

VAN OOYEN, A., VAN PELT, J., CORNER, M. A. & LOPES DA SILVA, F. H. (1982a). Long-lasting transients of activation in neural networks. *Neurocomputing* **4,** 75–87.

VAN OOYEN, A., VAN PELT, J., CORNER, M. A. & LOPES DA SILVA, F. H. (1992b). The emergence of long-lasting transients of activity in simple neural networks. *Biol. Cybern*. **67,** 269–277.

VAN OOYEN, A. (1994). Activity-dependent neural network development. *Network* **5,** 401–423.

VAN OOYEN, A. & VAN PELT, J. (1994a). Activity-dependent outgrowth of neurons and overshoot phenomena in developing neural networks. *J. theor. Biol*. **167,** 27–43.

VAN OOYEN, A. & VAN PELT, J. (1994b). Complex patterns of oscillations in a neural network model with activity-dependent outgrowth. In: *Artificial Neural Networks* 1, *Proceedings of the International Conference on Artificial Neural Networks*, *Sorrento* (*ICANN*'94) (Marinaro M. & Morasso, P. G., eds), pp. 146–149, Springer–Verlag.

VAN OOYEN, A., VAN PELT, J. & CORNER, M. A. (1995). Implications of activity-dependent neurite outgrowth for neuronal morphology and network development. *J. theor. Biol*. **172,** 63–82.

VAN OSS, C. & VAN OOYEN, A. (1995). Activity-dependent neurite outgrowth in a simple neural network model including excitation and inhibition. In: *Artificial Neural Networks*, *Proc*. 3*rd European Symp. on Artificial Neural Networks*, *Brussels* (*ESANN*'95), *D facto*, *Brussels* (Verleysen, M., ed.), pp. 87–92.